ACS Catalysis

pubs.acs.org/acscatalysis Research Article

Ruthenium(II)-Catalyzed Regioselective 1,2-Hydrosilylation of *N*-Heteroarenes and Tetrel Bonding Mechanism

Deepak Behera, Subramanian Thiyagarajan, Puthannur K. Anjalikrishna, Cherumuttathu H. Suresh,* and Chidambaram Gunanathan*

Cite This: *ACS Catal.* 2021, 11, 5885−5893 Read Online

ACCESS | Metrics & More | Article Recommendations | Supporting Information

ABSTRACT: An efficient regioselective dearomatization of *N*-heteroarenes using a ruthenium precatalyst [Ru-(*p*-cymene)(PCy_3)Cl_2] **1** is achieved. Reactions were performed under mild and neat conditions. A wide variety of *N*-heteroarenes undergo the addition of silanes in the presence of precatalyst **1**, leading to exclusive *N*-silyl-1,2-dihydroheteroarene products. This catalytic method displays a broad substrate scope; quinolines, isoquinolines, benzimidazoles, quinoxalines, pyrazines, pyrimidines, and pyridines undergo highly selective 1,2-dearomatization. Both electron-donating and electron-withdrawing substituents on *N*-heteroaromatics are well tolerated in this protocol. Mechanistic studies indicate the presence of [Ru-(*p*-cymene)(PCy_3)HCl] **4** in the reaction mixture, which may be the resting state of the catalyst. The complete catalytic cycle as revealed from density functional theory (DFT) studies show that the product formation is governed by N → Si tetrel bonding. Initially, PCy_3 dissociates from **1**, and further reaction of [(*p*-cymene)$RuCl_2$] **20** with silane generates the catalytically active intermediate [(*p*-cymene)RuHCl] **7**. Heteroarene coordinates with **7**, and subsequent dearomative 1,3-hydride transfer to the C2 position of the heteroaryl ligand generates an amide-ligated intermediate in which the reaction of silane occurs through a tetrel bonding and provides a selective pathway for 1,2-addition. DFT studies also revealed that ruthenium-catalyzed 1,4-hydroboration of pyridines is a facile process with a free energy barrier of 3.2 kcal/mol, whereas a pathway for the 1,2-hydroboration product is not observed due to the steric effects exerted by methyl groups on pinacolborane (HBpin) and *p*-cymene. Notably, enabled by the amine−amide inter-conversion of the coordinated heteroarene ligand, the +2 oxidation state of ruthenium intermediates remains unchanged throughout the catalytic cycle.

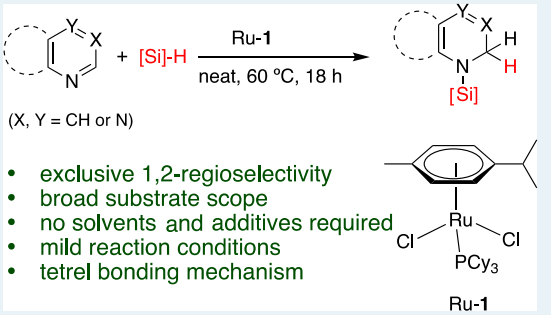

KEYWORDS: *hydrosilylation, ruthenium, 1,2-regioselectivity, N-heteroarenes, dearomatization, catalysis, tetrel bonding*

Downloaded via BUTLER UNIV on May 15, 2021 at 08:20:34 (UTC).
See https://pubs.acs.org/sharingguidelines for options on how to legitimately share published articles.

INTRODUCTION

Partial hydrogenation of *N*-heteroaromatic compounds is an essential strategy in synthetic chemistry because of their widespread application in the synthesis of natural products, bioactive molecules, and various drug molecules.[1] There are a number of biological transformations in which regioselective dearomatization occurs through oxidation or reduction reactions facilitated by microbes and enzymes present in nature.[2] Regioselective dearomatization of heteroaromatic compounds is a challenging task in synthetic chemistry due to the high resonance energy of aromatic rings and the formation of different regioisomers, and thus, it requires an efficient catalytic system to overcome these challenges.[3,4] In conventional organic synthesis, selective hydrogenation of *N*-heteroaromatic rings has been achieved using alkali metal hydrides, which suffers from serious drawbacks such as lack of selectivity, harsh reaction conditions, and generation of copious hazardous waste.[5] Hydrogenation reaction is the simplest and economical way to reduce aromatic rings. Unfortunately, hydrogenation of heteroaromatic molecules was performed under harsh conditions, which leads to over-reduction of aromatic rings and the formation of different regioisomers that are difficult to separate.[6] Alternatively, catalytic hydrogenation of quinolines is also achieved by using an excess amount of silanes and boranes, which resulted in over-reduction and provided tetrahydroquinoline products.[7] Thus, the development of transition-metal-catalyzed regioselective reduction of *N*-heteroaromatics under mild conditions is highly desirable.

The selective hydrosilylation and hydroboration of *N*-heteroarenes provide *N*-sila and bora-functionalized molecules, which are key intermediates for further functionalization. In the last decade, transition-metal-catalyzed regioselective hydroboration of *N*-heteroarenes is reported (Scheme 1).[8−10] However, hydroboration reaction on pyridine and quinoline

Received: March 12, 2021
Revised: April 16, 2021

© XXXX American Chemical Society

https://doi.org/10.1021/acscatal.1c01148
ACS Catal. 2021, 11, 5885−5893

Scheme 1. Catalytic Regioselective Hydroboration and Hydrosilylation of *N*-Heteroarenes

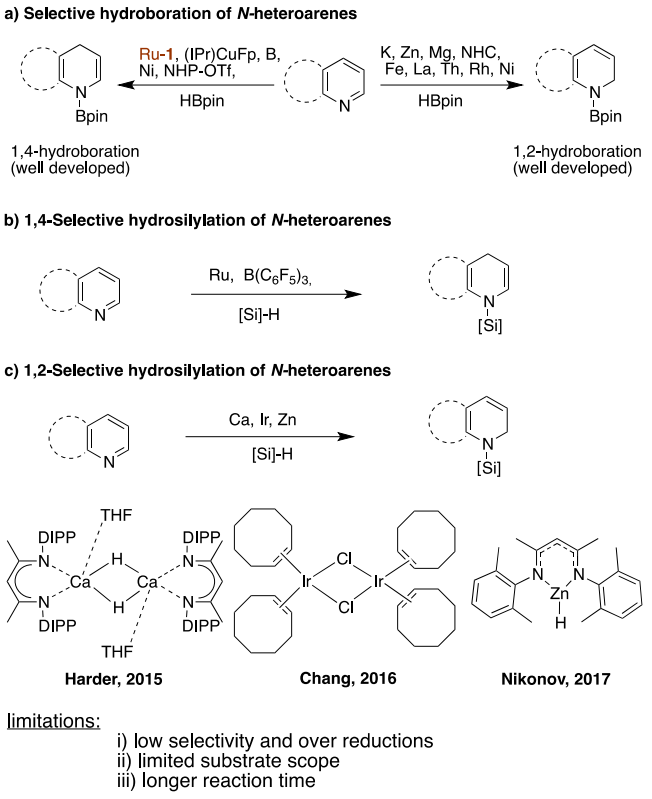

substrates provided a mixture of 1,2- and 1,4-addition products.[10] On the other hand, selective hydrosilylation of *N*-heteroaromatics also developed recently. Harrod and co-workers have reported the first homogeneous catalytic hydrosilylation of pyridines using titanium catalyst with moderate regioselectivity.[11] The groups of Nikonov and Oestreich have independently developed ruthenium-catalyzed 1,4-selective hydrosilylation of *N*-heteroarenes.[12,13] In contrast, 1,2-selective hydrosilylation of *N*-heteroarenes was less developed, and there are only three notable reports known in the literature. Harder and co-workers developed a calcium complex for catalytic regioselective dearomatization of pyridines with a limited substrate scope.[14] In 2016, Chang and co-workers reported an Ir(II)-catalyzed 1,2-hydrosilylation of *N*-heteroaromatic compounds.[15] Recently, Nikonov reported the Zn(II)-catalyzed hydrosilylation and hydroboration of *N*-heteroarenes with a narrow substrate scope and longer reaction time.[16] Very recently, the Wang group demonstrated 1,2-selective hydrogenation of quinolines using ammonia-borane as a reducing agent.[17] Despite these notable enticing signs of progress, the 1,2-selective hydrosilylation of *N*-heteroarenes remains underdeveloped. Thus, devising a new strategy under mild reaction conditions for regioselective 1,2-hydrosilylation of *N*-heteroaromatics is highly desirable.

We have reported catalytic hydroelementation reactions such as hydroboration of carbonyl compounds,[18] olefins,[19] deoxygenative hydroboration of carboxylic acids,[20] imines, and nitriles,[21] and also hydrosilylation of aldehydes,[22] using a readily available, simple dinuclear ruthenium complex $[Ru(p\text{-cymene})Cl_2]_2$. Using mono- and dinuclear ruthenium catalysts, multicomponent synthesis of borasiloxanes directly from pinacolborane, silane, and water was reported.[23] Using phosphine-ligated mononuclear ruthenium catalyst **1**, we have developed an efficient regioselective 1,4-hydroboration of pyridines.[24] Very recently, our group demonstrated the ruthenium-catalyzed selective hydroboronolysis of ethers.[25] In continuation of our interest in hydroelementation and selective dearomatization reactions, herein, we report the ruthenium-catalyzed regioselective 1,2-hydrosilylation of *N*-heteroaromatic compounds (Scheme 1). Surprisingly, a selectivity reversal from 1,4-addition to 1,2-addition is observed in the dearomatization of *N*-heteroarenes when electrophile changed from borane to silane. Mechanistic studies using density functional theory (DFT) calculations indicate that tetrel bonding is responsible for the observed selective 1,2-hydrosilylation of heteroaromatic compounds. To understand the origin of selectivity reversal, DFT studies were also performed on ruthenium-catalyzed hydroboration of pyridines. Notably, all the attempts to locate the transition state for 1,2-hydroboration of pyridine are failed, suggesting that the reaction is regioselective toward 1,4-addition of pinacolborane (HBpin) on pyridines as observed experimentally.[24] However, DFT calculations using a "reduced model" suggest that steric effects exerted by the methyl groups on HBpin and *p*-cymene are responsible for the regioselective 1,4-hydroboration of pyridines.

RESULTS AND DISCUSSION

Initial investigation on catalytic dearomatization by hydrosilylation was carried out using quinoline (0.5 mmol, 1 equiv) and phenylsilane (0.6 mmol, 1.2 equiv) in the presence of precatalyst **1** (2 mol %) at room temperature. After 12 h, ^{1}H NMR analysis of the reaction mixture indicated the selective formation of 1,2-hydrosilylation product **2a** in 78% yield (Table 1, entry 1). Increasing the reaction time to 24 h resulted in a significant improvement in the yield of **2a** (Table 1, entry 2). Quantitative formation of quinoline 1,2-hydrosilylation product **2a** was observed upon performing the reaction at 60 °C (Table 1, entry 3). When the phenylsilane was reduced to 1 equiv, the yield of **2a** diminished to 91% (Table 1, entry 4). Similarly, reducing catalyst load to 1 mol % also provided a lower yield (90%, Table 1, entry 5). The use of diethylsilane in this catalytic hydrosilylation reaction was tested, which provided product **2b** in quantitative yield (Table 1, entry 6). However, diphenylsilane failed to react (Table 1, entry 7). A control experiment was performed in the absence of a catalyst that confirmed the necessity of catalyst in this transformation (Table 1, entry 8).

Under the optimized reaction conditions, different quinoline derivatives were subjected to regioselective 1,2-hydrosilylation reactions, which are found to provide good to excellent yields (Scheme 2). Electron-donating groups such as methyl- and methoxy-substituted quinolines reacted with both phenylsilane and diethylsilane and delivered the products **2c−g** in quantitative yield with exclusive regioselectivity. Interestingly,

https://doi.org/10.1021/acscatal.1c01148
ACS Catal. 2021, 11, 5885−5893

Table 1. Optimization of the Reaction Conditions for the 1,2-Selective Hydrosilylation of Quinoline Catalyzed by 1[a]

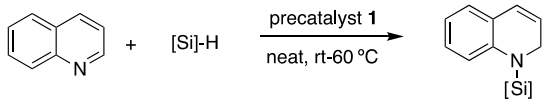

entry	1 (mol %)	silane (equiv)	temp (°C)	time (h)	yield (%)[b]
1	2	$PhSiH_3$ (1.2)	RT	12	78
2	2	$PhSiH_3$ (1.2)	RT	24	81
3	2	$PhSiH_3$ (1.2)	60	18	99
4	2	$PhSiH_3$ (1.0)	60	18	91
5	1	$PhSiH_3$ (1.2)	60	24	90
6	2	Et_2SiH_2 (1.5)	60	18	99
7	2	Ph_2SiH_2 (1.0)	60	18	n.r
8		$PhSiH_3$ (1.2)	60	18	n.r

[a]Reaction conditions: quinoline (0.5 mmol), silane, and precatalyst **1** were stirred at room temperature or 60 °C under closed conditions. [b]Yield was determined by ^{1}H NMR analysis of the reaction mixture using cyclohexane as an internal standard.

halogen-substituted quinolines were well tolerated in this reaction condition, which provided the products **2h−p** in excellent yields. However, the reaction is sensitive to the steric hindrance on quinolines. When 2-methyl quinoline and 8-methyl quinoline were reacted with phenylsilane, no reaction occurred. The reaction also tested with excess silane. However, no formation of products **2q** and **2r** was observed. Apparently, steric hindrance from the proximal methyl group adjacent to nitrogen in the ring prevented the reaction in these substrates. Also, 5-nitro quinoline was unsuccessful in this catalysis due to the solubility problem.

To diversify ruthenium-catalyzed regioselective 1,2-hydrosilylation using precatalyst **1,** various *N*-heteroarenes were subjected in this catalytic protocol (Scheme 3). Substituted pyridines such as 3-methylpyridine, 3-methoxypyridine, and 4-benzylpyridine underwent exclusive 1,2-dearomatization and provided products **3a−c** in 41, 85, and 50% yields, respectively. The reaction of 3-pyridyl acetate resulted in the mixture of products with incomplete conversion of the starting material due to the presence of sensitive and competing ester functionality. When pyrazine was reacted under the standard condition with diethylsilane, regioselective 1,2-hydrosilylation occurred on both nitrogen centers, leading to the formation of 1,2,3,4-tetrahydropyrazine product **3d** in 40% yield. Notably, 2-methyl pyrazine provided regioselective double-1,2-hydrosilylation product **3e** in quantitative yield. 4-Methyl pyrimidine also underwent double hydrosilylation (**3f,** 81% yield). Benzo-fused five-member heterocycle 1-methylbenzimidazole provided 1,2-hydrosilylation product **3g** quantitatively. When isoquinoline was reacted with diethylsilane, regioselective 1,2-hydrosilylation product **3h** was obtained in quantitative yield; however, a similar reaction with phenylsilane exclusively resulted in the formation of bis(dihydroisoquinoline) product **3m**. The formation of such double-addition product with isoquinoline was also observed in other catalytic systems.[10b,14] Remarkably, contrary to the 2-methylquinoline, 1-methyl isoquinoline reacted with diethylsilane, and exclusive 1,2 hydrosilylation product **3i** was observed in which 1,2-addition occurred on nitrogen and methyl-substituted aryl carbon (see **2q** in Schemes 2 and 3). In the case of quinoxaline and 6-chloro quinoxaline, quantitative formation of products **3j** and **3k** occurred. The reaction of acridine with phenylsilane

Scheme 2. Ruthenium-Catalyzed 1,2-Selective Hydrosilylation of Quinolines[a]

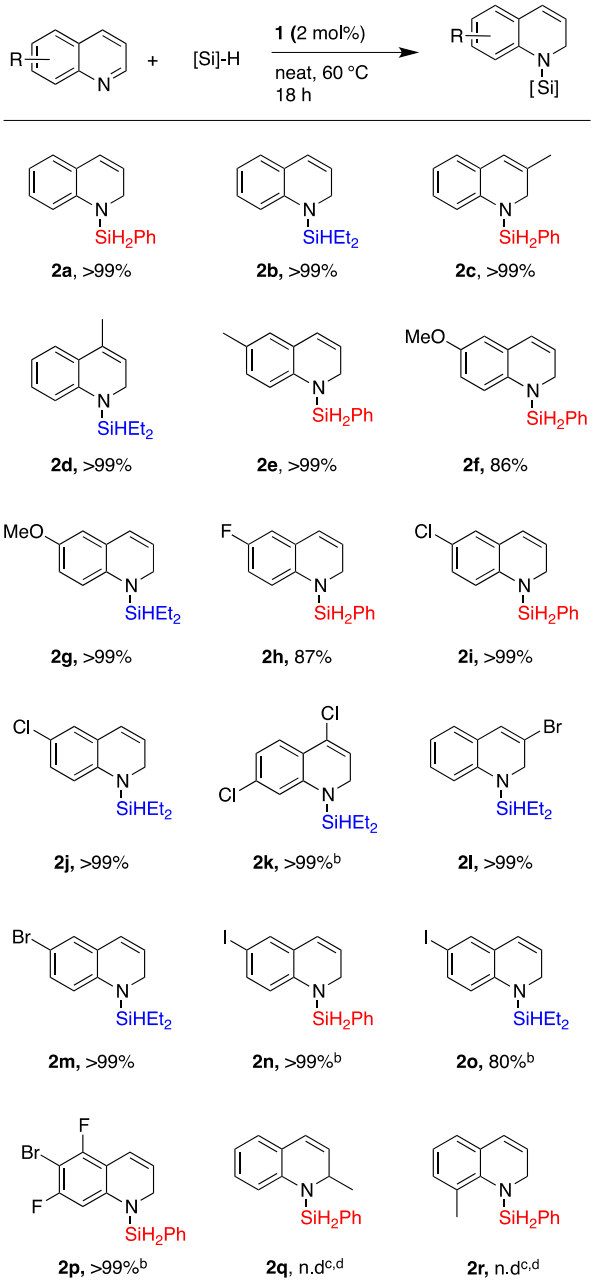

[a]Reaction conditions: substrate (0.5 mmol, 1 equiv), $PhSiH_3$ (0.6 mmol, 1.2 equiv), or Et_2SiH_2 (0.75 mmol, 1.5 equiv) and precatalyst **1** (2 mol%) were stirred at 60 °C for 18 h. The yield was calculated by ^{1}H NMR analysis using cyclohexane as an internal standard. [b]$CDCl_3$ (0.3 mL) was used. [c]2 equiv of $PhSiH_3$ was used. [d]Not detected.

provided 1,4-addition product **3l** exclusively with 83% yield, as 1,2-addition is not favored on this substrate.

Toward understanding the reaction mechanism, a stoichiometric experiment using precatalyst **1** with phenylsilane (5 equiv) was carried out, and the reaction was monitored by NMR spectroscopy. The ^{1}H NMR spectrum of the reaction mixture was recorded after 15 min, showing the formation of ruthenium monohydride intermediate **4**, which resonated a characteristic doublet at δ −7.84 ppm (J_{PH} = 49.2 Hz) as well as a doublet at δ 59.70 ppm (J_{PH} = 50.6 Hz) in ^{31}P NMR

https://doi.org/10.1021/acscatal.1c01148
ACS Catal. 2021, 11, 5885−5893

Scheme 3. Ruthenium-Catalyzed Regioselective 1,2-Hydrosilylation of *N*-Heterocycles[a]

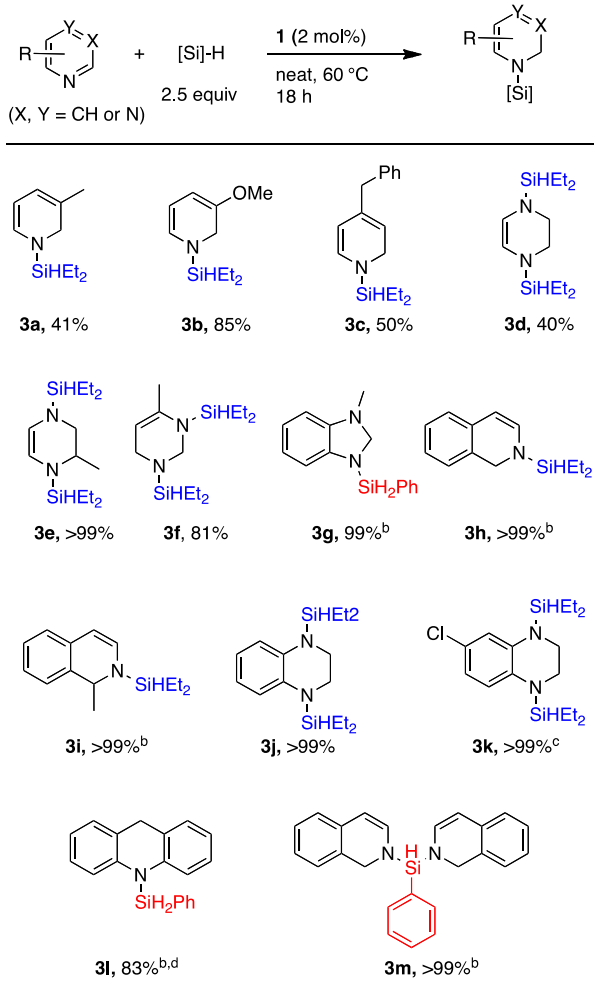

[a]Reaction conditions: substrate (0.5 mmol, 1 equiv), silane (1.25 mmol, 2.5 equiv), and 2 mol% of precatalyst **1** were stirred at 60 °C for 18 h and the yield was calculated by ^{1}H NMR analysis using cyclohexane as an internal standard. [b]1.5 equiv of silane was used. [c]Reaction performed using 0.3 mL of $CDCl_3$. [d]C_6D_6 (0.3 mL) was used.

Scheme 4. Mechanistic Investigations for Ruthenium-Catalyzed Regioselective 1,2-Hydrosilylation of *N*-Heteroarenes

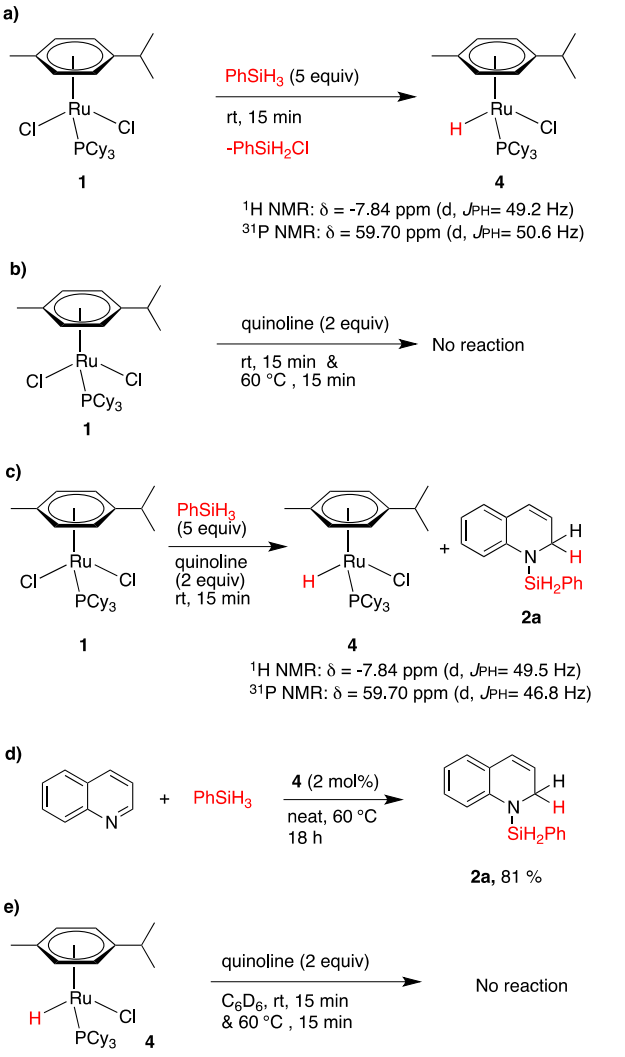

(Scheme 4a). Unfortunately, repeated experiments were performed to obtain the single crystals for X-ray analysis of complex **4**, which remained unsuccessful so far. When precatalyst **1** reacted with quinoline (2 equiv), no reaction was observed (^{1}H and ^{31}P NMR) after 15 min both at room temperature and at 60 °C (Scheme 4b). Reaction of catalyst **1** with phenylsilane (5 equiv) and quinoline (2 equiv) resulted in the same ruthenium hydride intermediate **4** (observed after 15 min) in NMR analysis: ^{1}H NMR doublet at δ −7.84 ppm (J_{PH} = 49.5 Hz) as well as in ^{31}P NMR doublet at δ 59.70 ppm (J_{PH} = 46.8 Hz) and formation of product **2a** (Scheme 4c). When intermediate **4** employed as a catalyst, the formation of desired 1,2-hydrosilylation product **2a** was observed in 81% yield under standard reaction conditions. This experiment indicates the involvement of Ru−H intermediate in the catalytic hydrosilylation of heteroarenes (Scheme 4d). The reaction of isolated intermediate **4** with quinoline in the absence of silane was performed (Scheme 4e). The ^{1}H NMR spectrum of the crude reaction mixture indicated the absence of 1,3-hydride shift on quinoline, which indicates the necessity of silane to attain these dearomatization reactions. Further, the reaction was also monitored by ^{31}P NMR; no signals that correspond to quinoline-coordinated ruthenium intermediate or dissociation of chloride ligands were observed. Only a minor amount of dissociated free phosphine ligand (PCy_3) from catalyst **4** was observed.

^{1}H NMR monitoring of this reaction indicated the persistence of the intermediate **4** throughout the reaction (Figure 1). These experiments indicate the facile reaction of silane with precatalyst **1** to provide intermediate **4,** which may be a catalyst resting state. Notably, while precatalyst **1** does not react with quinoline directly, it reacts with silane to provide the intermediate **4**, which then reacts with quinoline in the presence of silane, leading to the formation of regioselective 1,2-addition product.

Further, a plausible mechanism for the reaction[26] is derived using DFT calculation at M06L/BS1/SMD level,[27] where BS1 stands for a mixed basis set (LanL2DZ for Ru and 6-31G** for other atoms). At first, PCy_3 dissociation from [Ru-(*p*-cymene)(PCy_3)Cl_2] **1** is invoked to produce the active dichloro complex.[28] The dissociation occurs with a free energy change of 14.6 kcal/mol. The Si−H bond of $PhSiH_3$ interacts with the

https://doi.org/10.1021/acscatal.1c01148
ACS Catal. 2021, 11, 5885−5893

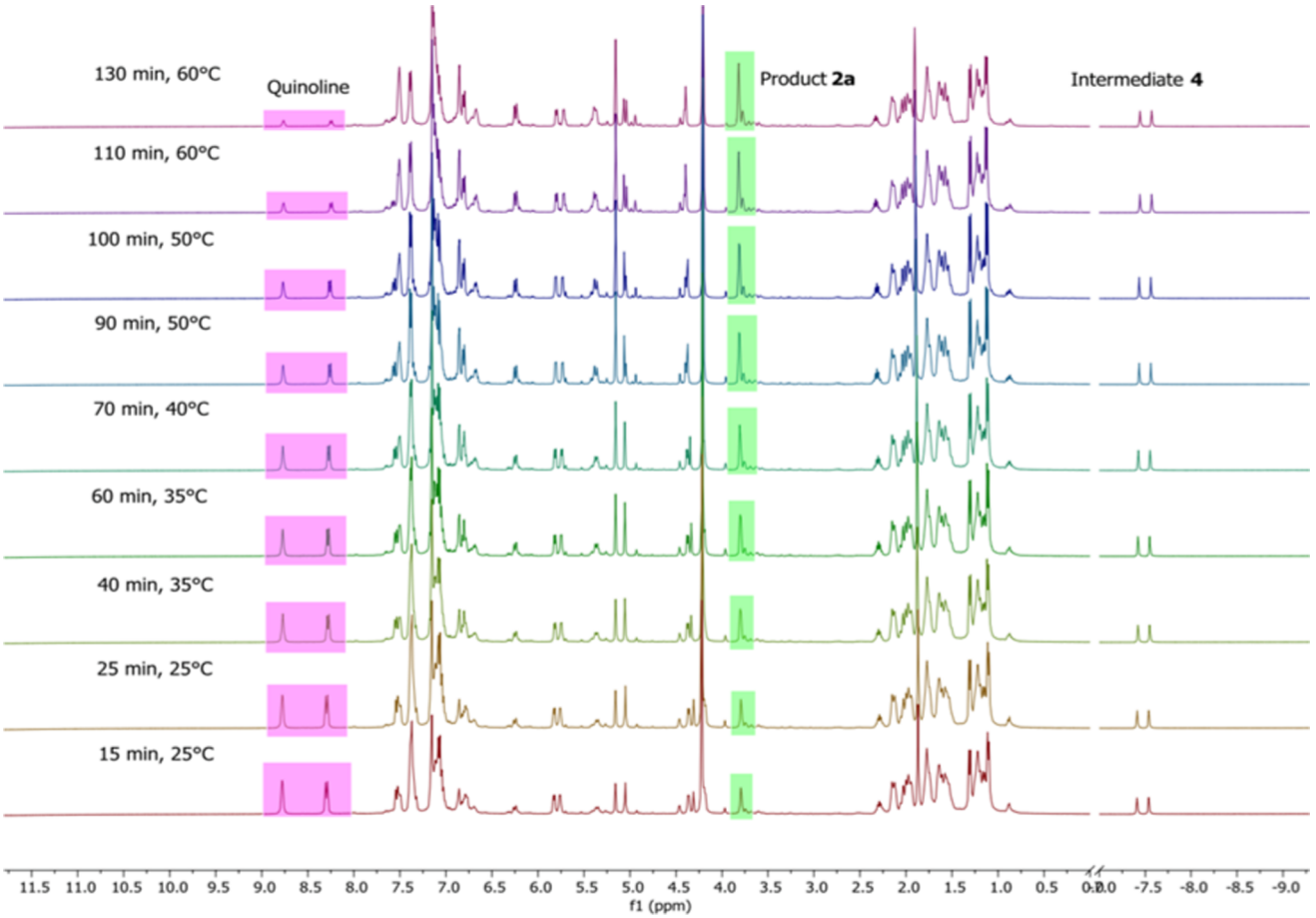

Figure 1. ^{1}H NMR monitoring: the stoichiometric reaction of quinoline with phenylsilane and precatalyst **1**.

Ru(II) center of [Ru-(*p*-cymene)Cl_2] to yield the intermediate **5** (Figure 2). **TS1** represents a four-center transition state for an exchange reaction, which describes the transition of hydride from silicon to ruthenium along with the simultaneous transfer of chloride from ruthenium to silicon. The activation free energy ($\Delta G^{\#}$) for the chloro-hydride ligand exchange is 27.8 kcal/mol. The intermediate **6** formed at this step has a weak interaction between the chloro of silylchloride and Ru(II). An active hydride complex [Ru-(*p*-cymene)HCl] (**7**) is formed by the dissociation of chlorophenylsilane (**8**) from **6**. Notably, intermediate **7** was observed in mass spectral analysis, and we have previously established its involvement in the anti-Markovnikov hydroboration of alkenes.[19]

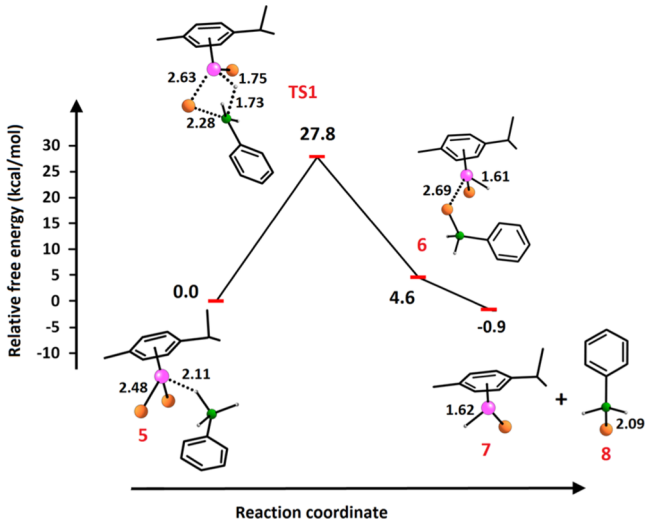

Figure 2. Ru(II)chloride to Ru(II) hydride exchange reaction.

The second stage of the reaction occurs when the 16-electron complex **7** gets coordinated with an *N*-heteroaromatic system such as quinoline, leading to the formation of **9** with the coordination free energy −9.5 kcal/mol. The hydride migration (1,3-hydride shift) to ortho position of quinoline is feasible for **9** by passing through **TS2** with $\Delta G^{\#}$ 21.1 kcal/mol (Figure 3). The 16-electron Ru(II) complex **10** could be coordinated with PCy3, or it may undergo further reaction with $PhSiH_3$.

The third stage of the reaction considers the formation of complex **11** (Figure 4). In **11**, one of the Si−H bonds shows a significant interaction with the ruthenium center. Also, the Si−N distance at 1.96 Å suggests noncovalent tetrel bonding between Si and N. The σ-donation from the lone pair electrons on the *N*-center of dihydroquinoline in **10** to the hole region in phenylsilane leads to tetrel bonding (Figure 5). The hypervalent penta-coordinate characteristic[29] is developed on Si in **11** with the typical trigonal bipyramidal geometry.[29] The Si−H bond of **11** cleaves by liberating a hydride ligand to the metal center (**12**) through an early transition state **TS3** with $\Delta G^{\#}$ 2.3 kcal/mol. The Si atom in **TS3** mimics the characteristics of the central atom of an S_N2 type transition state. The very low barrier for the Si−H bond cleavage can be attributed to the N → Si tetrel bonding interaction in **TS3**. In **12**, *N*-silyl-1,2-

https://doi.org/10.1021/acscatal.1c01148
ACS Catal. 2021, 11, 5885−5893

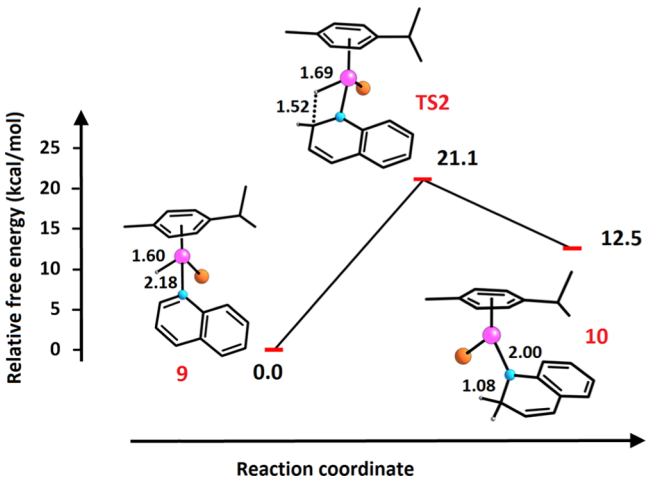

Figure 3. Mechanism for a 1,3-hydride shift.

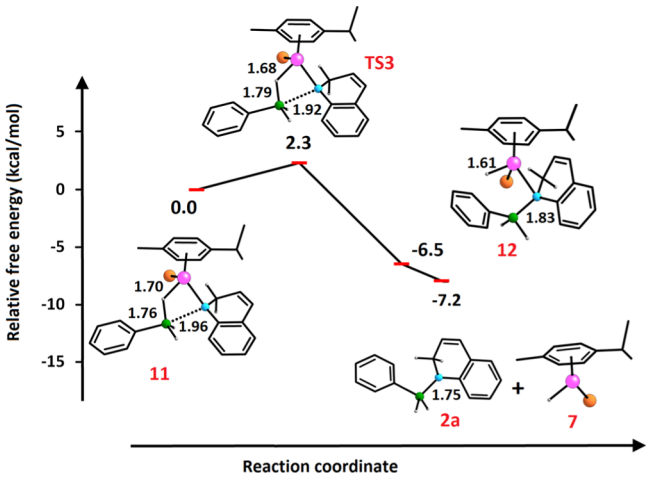

Figure 4. Mechanism for the hydrosilylation of quinoline driven by tetrel bonding.

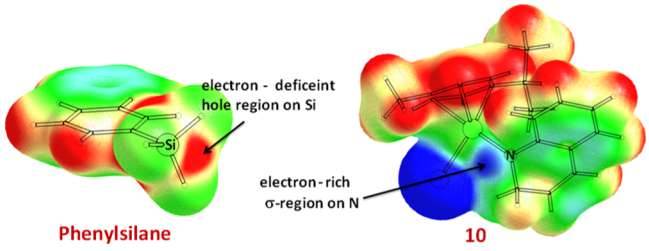

Figure 5. Hole and σ regions for tetrel bonding: illustration using molecular electrostatic potential on electron density iso-surface 0.006 a.u.

dihydroquinoline (**2a**) is coordinated with [Ru-(*p*-cymene)-HCl], **7**. Dissociation of **2a**, the final product from **12**, liberates the catalytically active hydride complex [Ru-(*p*-cymene)HCl], **7**. Ru remains in +2 oxidation state throughout the catalytic cycle, and *p*-cymene ligand adopts the hapticity η6. In the figures, magenta, orange, green, and aqua blue are Ru, Cl, Si, and N, respectively.

Tetrel bonding is considered as a powerful noncovalent bonding between electron donors and the carbon group 14 elements where the positive electrostatic potential is localized over the tetrel atom.[30] In a recent review, Guedes da Silva et al. have discussed the importance of tetrel bonding and other noncovalent interactions in metal complex catalysis.[31] The existence of neutral penta-, hexa-, and even hepta-coordinated species containing N → Si dative bonding[32] is reported in the literature in the fields of crystal engineering and supramolecular chemistry.[33,34] The significance of tetrel bonding in the Ru(II)-catalyzed hydrosilylation of *N*-heteroarenes is revealed for the first time here. Figure 4 can be regarded as one of the rare examples of a "tetrel bonding energy profile", which connects the tetrel-bonded reactant, TS and product.

Previously, Gunanathan et al. reported the [Ru(*p*-cymene)-$Cl_2(P(Cy)_3)$]-catalyzed regioselective 1,4-hydroboration of pyridines using pinacolborane (HBpin).[24] A DFT study on the mechanism of this reaction is performed to compare it with the regioselective 1,2-hydrosilylation of heteroarenes. The active form of the catalyst for the 1,4-hydroboration is expected to be [Ru(*p*-cymene)Cl_2], formed by the dissociation of the bulky PCy_3 ligand from the catalyst. Similar to **5**, the Ru(II) dichloro species forms an adduct with HBpin with a binding energy of −5.9 kcal/mol. In the adduct, one of the chloro ligands is exchanged for the hydride group of HBpin, resulting in the formation of Ru(II)hydrido complex [Ru(*p*-cymene)HCl] and ClBpin (Figure 6). The $\Delta G^{\#}$ for the

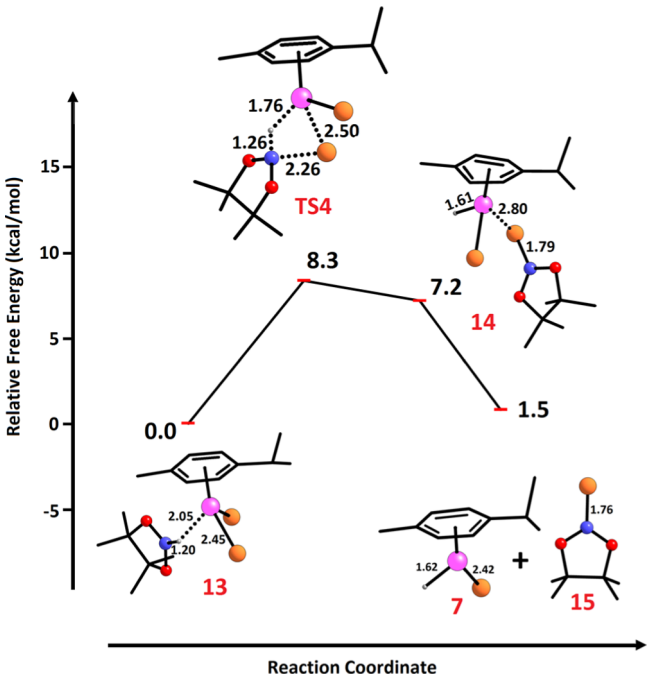

Figure 6. Ru(II) chloride to Ru(II) hydride exchange reaction.

reaction is found to be 8.3 kcal/mol, much lower than that required for a similar exchange reaction given in Figure 2 for the hydrosilylation reaction. The reaction is endergonic by 1.5 kcal/mol. Both HBpin and ClBpin can form a zwitterionic adduct with pyridine by the coordinate N → B bonding interaction. The HBpin...Py complex **16** formation is endergonic (4.7 kcal/mol) with a complexation energy of −8.4 kcal/mol, whereas ClBpin...Py complex **17** formations showed exergonic characteristic (1.6 kcal/mol) with a complexation energy of −15.2 kcal/mol (Figure S1; Supporting Information). Since the energetics support the spontaneous formation of ClBpin...Py complex, we assume that this adduct reacts with the [Ru(*p*-cymene)HCl] complex. The Cl of ClBpin...Py is anionic in nature and coordinates with Ru(II) to yield the

https://doi.org/10.1021/acscatal.1c01148
ACS Catal. 2021, 11, 5885−5893

complex **18** as given in Figure 7. The chloro unit migrates to Ru(II) with the simultaneous exchange of hydride ligand from

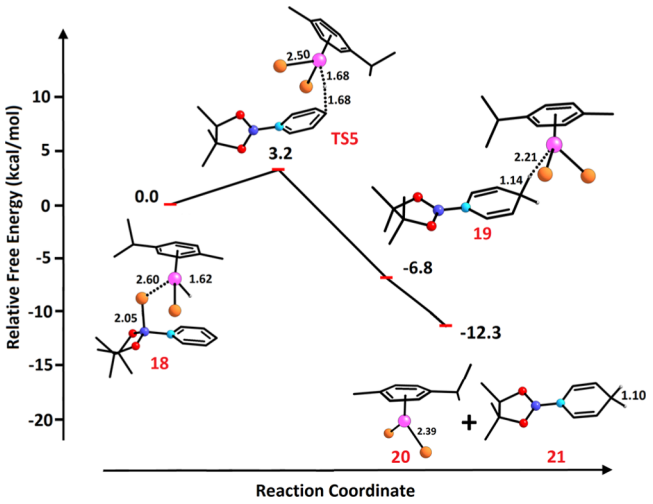

Figure 7. Mechanism for the hydroboration of pyridine.

Ru(II) to the fourth position of pyridine. The transition state for this reaction is depicted in Figure 7, and the free energy barrier is found to be 3.2 kcal/mol. The products of the reaction are 1,4-dihydropyridine adduct of HBpin and the active form of the catalyst is [Ru(*p*-cymene)Cl_2]. The reaction is exergonic by 12.3 kcal/mol. All attempts to locate a transition state for the formation of 1,2-dihydropyridine adduct of HBpin is failed, suggesting that the reaction is regioselective toward 1,4-hydroboration of the pyridine. It may be noted that when we conducted a study by substituting all methyl groups in HBpin by H and also used benzene moiety instead of *p*-cymene for the metal complex, we could locate a transition state for the 1,2-hydroboration product, which showed lower barrier height than the 1,4-hydroboration reaction. The results from this "reduced" model suggest that steric effects exerted by the methyl groups of HBpin and *p*-cymene units are responsible for the promotion of the regioselective 1,4-hydroboration reactions.

On the basis of experimental observations, DFT calculations, and our previous reports on catalytic hydroboration and hydrosilylation of different functional groups,[18−25] the plausible reaction mechanism for regioselective 1,2-hydrosilylation of *N*-heteroaromatic compounds is proposed in Scheme 5. DFT studies indicate the dissociation of phosphine ligand from the catalyst **1**, leading to the formation of dichloro ruthenium intermediate **20**, which upon reaction with phenylsilane generates **7**. Further quinoline coordination to **7** results in **9**, which then undergoes intramolecular dearomative 1,3-hydride transfer to the C2 position of the heteroaryl ligand to produce the Ru-amide intermediate **10**. The reaction of **10** with silane occurs via unique tetrel bonding and results in Si−H and Ru interaction, and subsequent sigma bond metathesis in **11** leads to the formation of amine coordinated Ru monohydride species **12**. The dissociation of 1,2-hydrosilylation product (**2a**) from **12** regenerates the catalytically active intermediate **7** and completes one loop in a catalytic cycle. The reaction of complex **1** with phenylsilane leads to the formation of ruthenium hydride intermediate **4** as observed by ^{1}H NMR analysis (Scheme 4a), and the presence of **4** is also observed throughout the catalysis on monitoring the reaction

Scheme 5. Proposed Catalytic Cycle for Regioselective 1,2-Hydrosilylation of *N*-Heteroarenes and Free Energy Changes

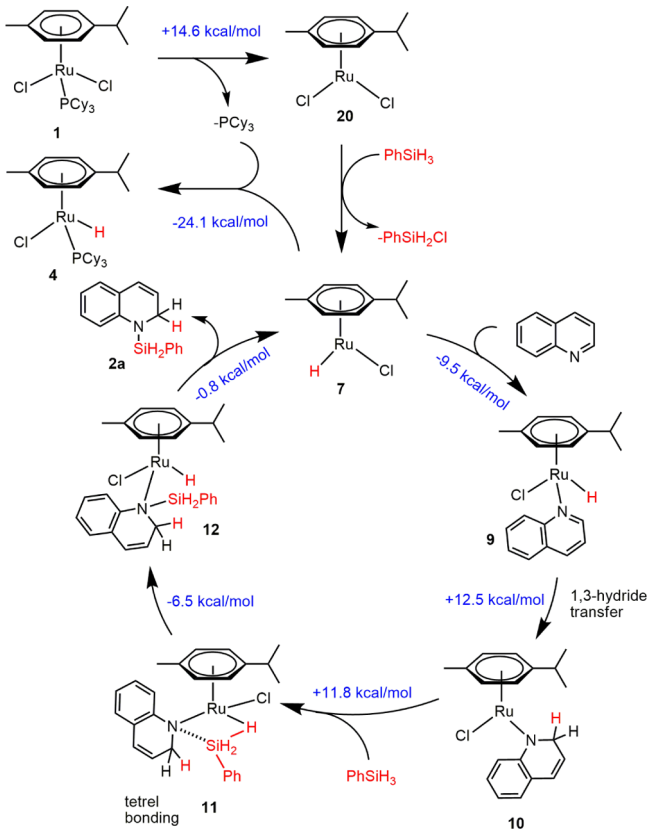

progress, indicating perhaps that it could be a catalyst resting state. Notably, all the ruthenium intermediates in the catalytic cycle remain in +2 oxidation state, which is enabled by the in situ interconversion of amine−amide ligation of heteroaromatic motifs.

CONCLUSIONS

In summary, a highly regioselective method for 1,2-dearomative hydrosilylation of *N*-heteroarenes using the simple and readily accessible ruthenium precatalyst **1** is reported. Various *N*-heteroarenes are subjected to catalysis under this condition, and the corresponding regioselective 1,2-hydrosilylation products are observed in good to excellent yields with exclusive selectivity. The formation of a PCy_3-coordinated Ru−H intermediate **4** was identified from a stoichiometric experiment, which may be regarded as the resting state of the catalyst. DFT studies indicate that dissociation of PCy_3 from **4** yields the catalytically active complex [Ru-(*p*-cymene)HCl] **7**, which upon coordination with quinoline leads to the 1,3-hydride transfer reaction. The amide complex formed in the reaction undergoes N → Si tetrel bonding with the phenylsilane to yield the *N*-silyl-1,2-dihydroquinoline. On the contrary, the steric effects exerted by the methyl groups on HBpin and *p*-cymene coordinated with ruthenium are found to be responsible for 1,4-hydroboration of pyridines catalyzed by the same precatalyst **1**. Remarkably, this selective catalytic hydrosilylation of *N*-heteroarenes proceeds under neat, activator-free, and mild reaction conditions, which make the protocol complete atom economical and environmentally benign.

https://doi.org/10.1021/acscatal.1c01148
ACS Catal. 2021, 11, 5885−5893

■ ASSOCIATED CONTENT

Supporting Information

The Supporting Information is available free of charge at https://pubs.acs.org/doi/10.1021/acscatal.1c01148.

Experimental procedures, spectral data, copies of ^{1}H and ^{13}C NMR spectra of the products, and computational data (PDF)

■ AUTHOR INFORMATION

Corresponding Authors

Cherumuttathu H. Suresh − *Chemical Sciences and Technology Division, CSIR-National Institute for Interdisciplinary Science and Technology, Thiruvananthapuram 695019, India; Academy of Scientific and Innovative Research (AcSIR), Ghaziabad 201002, India;* orcid.org/0000-0001-7237-6638; Email: sureshch@gmail.com

Chidambaram Gunanathan − *School of Chemical Sciences, National Institute of Science Education and Research, HBNI, Bhubaneswar 752050, India;* orcid.org/0000-0002-9458-5198; Email: gunanathan@niser.ac.in

Authors

Deepak Behera − *School of Chemical Sciences, National Institute of Science Education and Research, HBNI, Bhubaneswar 752050, India*

Subramanian Thiyagarajan − *School of Chemical Sciences, National Institute of Science Education and Research, HBNI, Bhubaneswar 752050, India;* orcid.org/0000-0002-0735-5686

Puthannur K. Anjalikrishna − *Chemical Sciences and Technology Division, CSIR-National Institute for Interdisciplinary Science and Technology, Thiruvananthapuram 695019, India; Academy of Scientific and Innovative Research (AcSIR), Ghaziabad 201002, India*

Complete contact information is available at: https://pubs.acs.org/10.1021/acscatal.1c01148

Notes

The authors declare no competing financial interest.

■ ACKNOWLEDGMENTS

C.G. thanks SERB New Delhi (EMR/2016/002517), DAE, and NISER for financial support. D.B. thanks DST for an inspire fellowship. S.T. thanks UGC for a research fellowship. C.H.S. is grateful to CSIR for funding. P.K.A. is thankful to UGC, Government of India, for providing Senior Research Fellowship.

■ DEDICATION

Dedicated to Prof. T. K. Chandrashekar on the occasion of his 65th birthday with our best wishes.

■ REFERENCES

(1) (a) Park, S.; Chang, S. Catalytic Dearomatization of N-Heteroarenes with Silicon and Boron Compounds. *Angew. Chem., Int. Ed.* **2017**, *56*, 7720−7738. (b) Liu, Z.; Chen, L.; Li, J.; Liu, K.; Zhao, J.; Xu, M.; Feng, L.; Wan, R.-z.; Li, W.; Liu, L. Oxidative C-H Functionalization of N-Carbamoyl 1,2-Dihydroquinolines. *Org. Biomol. Chem.* **2017**, *15*, 7600−7606. (c) Welsch, M. E.; Snyder, S. A.; Stockwell, B. R. Privileged Scaffolds for Library Design and Drug Discovery. *Curr. Opin. Chem. Biol.* **2010**, *14*, 347−361. (d) Michael, J. P. Quinoline, Quinazoline and Acridone Alkaloids. *Nat. Prod. Rep.* **2000**, *17*, 603−620.

(2) (a) Kung, J. W.; Baumann, S.; Von Bergen, M.; Müller, M.; Hagedoorn, P.-L.; Hagen, W. R.; Boll, M. Reversible Biological Birch Reduction at an Extremely Low Redox Potential. *J. Am. Chem. Soc.* **2010**, *132*, 9850−9856. (b) Thiele, B.; Rieder, O.; Golding, B. T.; Müller, M.; Boll, M. Mechanism of Enzymatic Birch Reduction: Stereochemical Course and Exchange Reactions of Benzoyl-CoA Reductase. *J. Am. Chem. Soc.* **2008**, *130*, 14050−14051. (c) Boll, M. Dearomatizing Benzene Ring Reductases. *J. Mol. Microbiol. Biotechnol.* **2005**, *10*, 132−142.

(3) (a) Balaban, A. T.; Oniciu, D. C.; Katritzky, A. R. Aromaticity as a Cornerstone of Heterocyclic Chemistry. *Chem. Rev.* **2004**, *104*, 2777−2812. (b) Krygowski, T. M.; Cyrański, M. K. Structural Aspects of Aromaticity. *Chem. Rev.* **2001**, *101*, 1385−1420.

(4) (a) Bull, J. A.; Mousseau, J. J.; Pelletier, G.; Charette, A. B. Synthesis of Pyridine and Dihydropyridine Derivatives by Regio- and Stereoselective Addition to *N*-Activated Pyridines. *Chem. Rev.* **2012**, *112*, 2642−2713. (b) Lavilla, R. Recent Developments in the Chemistry of Dihydropyridines. *J. Chem. Soc., Perkin Trans. 1* **2002**, 1141−1156.

(5) (a) Donohoe, T. J.; McRiner, A. J.; Sheldrake, P. Partial Reduction of Electron-Deficient Pyridines. *Org. Lett.* **2000**, *2*, 3861−3863. (b) Birch, A. J.; Karakhanov, E. A. Preparation of some N-Substituted 1,4-Dihydropyridines by Metal-Ammonia Reactions. *J. Chem. Soc., Chem. Commun.* **1975**, 480−481. (c) Danishefsky, S.; Cain, P.; Nagel, A. Bis Annelations via 6-methyl-2-vinylpyridine. Efficient Synthesis of dl-D-Homoestrone. *J. Am. Chem. Soc.* **1975**, *97*, 380−387. (d) Danishefsky, S.; Cain, P. Pyridine Route to .alpha.-Substituted Cyclohexenones. *J. Org. Chem.* **1975**, *40*, 3606−3608. (e) Danishefsky, S.; Cavanaugh, R. Bis Annelation with 6-vinyl-2-picoline. *J. Am. Chem. Soc.* **1968**, *90*, 520−521.

(6) (a) Takasaki, M.; Motoyama, Y.; Higashi, K.; Yoon, S.-H.; Mochida, I.; Nagashima, H. Ruthenium Nanoparticles on Nano-Level-Controlled Carbon Supports as Highly Effective Catalysts for Arene Hydrogenation. *Chem.—Asian J.* **2007**, *2*, 1524−1533. (b) Freifelder, M. *Practical Catalytic Hydrogenation*; Wiley Interscience, 1971; pp 1−663. (c) Glorius, F. Asymmetric Hydrogenation of Aromatic Compounds. *Org. Biomol. Chem.* **2005**, *3*, 4171−4175. (d) Lunn, G.; Sansone, E. B. Facile reduction of pyridines with nickel-aluminum alloy. *J. Org. Chem.* **1986**, *51*, 513−517. (e) Freifelder, M.; Stone, G. R. Reductions with Ruthenium. II. Its Use in the Hydrogenation of Pyridines. *J. Org. Chem.* **1961**, *26*, 3805−3808. (f) Adkins, H.; Kuick, L. F.; Farlow, M.; Wojcik, B. Hydrogenation of Derivatives of Pyridine. *J. Am. Chem. Soc.* **1934**, *56*, 2425−2428.

(7) (a) Yang, C.-H.; Chen, X.; Li, H.; Wei, W.; Yang, Z.; Chang, J. Iodine Catalyzed Reduction of Quinolines under Mild Reaction Conditions. *Chem. Commun.* **2018**, *54*, 8622−8625. (b) Gandhamsetty, N.; Joung, S.; Park, S.-W.; Park, S.; Chang, S. Boron-Catalyzed Silylative Reduction of Quinolines: Selective sp3 C-Si Bond Formation. *J. Am. Chem. Soc.* **2014**, *136*, 16780−16783.

(8) (a) Yu, H.-C.; Islam, S. M.; Mankad, N. P. Cooperative Heterobimetallic Substrate Activation Enhances Catalytic Activity and Amplifies Regioselectivity in 1,4-Hydroboration of Pyridines. *ACS Catal.* **2020**, *10*, 3670−3675. (b) Liu, T.; He, J.; Zhang, Y. Regioselective 1,2-Hydroboration of *N*-Heteroarenes Using a Potassium-Based Catalyst. *Org. Chem. Front.* **2019**, *6*, 2749−2755. (c) Tamang, S. R.; Singh, A.; Unruh, D. K.; Findlater, M. Nickel-Catalyzed Regioselective 1,4-Hydroboration of N-Heteroarenes. *ACS Catal.* **2018**, *8*, 6186−6191. (d) Rao, B.; Chong, C. C.; Kinjo, R. Metal-free Regio- and Chemoselective Hydroboration of Pyridines Catalyzed by 1,3,2-Diazaphosphenium Triflate. *J. Am. Chem. Soc.* **2018**, *140*, 652−656. (e) Zhang, F.; Song, H.; Zhuang, X.; Tung, C.-H.; Wang, W. Iron-Catalyzed 1,2-Selective Hydroboration of N-Heteroarenes. *J. Am. Chem. Soc.* **2017**, *139*, 17775−17778. (f) Fan, X.; Zheng, J.; Li, Z. H.; Wang, H. Organoborane Catalyzed Regioselective 1,4-Hydroboration of Pyridines. *J. Am. Chem. Soc.* **2015**, *137*, 4916−4919. (g) Dudnik, A. S.; Weidner, V. L.; Motta, A.; Delferro, M.; Marks, T. J. Atom-Efficient Regioselective 1,2-Dearomatization of

Functionalized Pyridines by an Earth-Abundant Organolanthanide Catalyst. *Nat. Chem.* **2014**, *6*, 1100−1107. (h) Oshima, K.; Ohmura, T.; Suginome, M. Regioselective Synthesis of 1,2-Dihydropyridines by Rhodium-Catalyzed Hydroboration of Pyridines. *J. Am. Chem. Soc.* **2012**, *134*, 3699−3702.

(9) After initial submission of this manuscript, notable regioselective hydroboration of N-heteroaromatics are reported. (a) Liu, X.; Li, B.; Hua, X.; Cui, D. 1,2-Hydroboration of Pyridines by Organomagnesium. *Org. Lett.* **2020**, *22*, 4960−4965. (b) Jeong, J.; Heo, J.; Kim, D.; Chang, S. NHC-Catalyzed 1,2-Selective Hydroboration of Quinolines. *ACS Catal.* **2020**, *10*, 5023−5029.

(10) (a) Chatterjee, B.; Gunanathan, C. Catalytic Dearomative Hydroboration of Heteroaromatic Compounds. *J. Chem. Sci.* **2019**, *131*, 118. (b) Wang, X.; Zhang, Y.; Yuan, D.; Yao, Y. Regioselective Hydroboration and Hydrosilylation of N-Heteroarenes Catalyzed by a Zinc Alkyl Complex. *Org. Lett.* **2020**, *22*, 5695−5700. (c) Zhang, Z.; Huang, S.; Huang, L.; Xu, X.; Zhao, H.; Yan, X. Synthesis of Mesoionic N-Heterocyclic Olefins and Catalytic Application for Hydroboration Reactions. *J. Org. Chem.* **2020**, *85*, 12036−12043. (d) Liu, J.; Chen, J.-Y.; Jia, M.; Ming, B.; Jia, J.; Liao, R.-Z.; Tung, C.-H.; Wang, W. Ni-O Cooperation versus Nickel(II) Hydride in Catalytic Hydroboration of *N*-Heteroarenes. *ACS Catal.* **2019**, *9*, 3849−3857. (e) Intemann, J.; Lutz, M.; Harder, S. Multinuclear Magnesium Hydride Clusters: Selective Reduction and Catalytic Hydroboration of Pyridines. *Organometallics* **2014**, *33*, 5722−5729. (f) Arrowsmith, M.; Hill, M. S.; Hadlington, T.; Kociok-Köhn, G.; Weetman, C. Magnesium-Catalyzed Hydroboration of Pyridines. *Organometallics* **2011**, *30*, 5556−5559.

(11) Hao, L.; Harrod, J. F.; Lebuis, A.-M.; Mu, Y.; Shu, R.; Samuel, E.; Woo, H.-G. Homogeneous Catalytic Hydrosilylation of Pyridines. *Angew. Chem., Int. Ed.* **1998**, *37*, 3126−3129.

(12) (a) Lee, S.-H.; Gutsulyak, D. V.; Nikonov, G. I. Chemo- and Regioselective Catalytic Reduction of *N*-Heterocycles by Silane. *Organometallics* **2013**, *32*, 4457−4464. (b) Gutsulyak, D. V.; van der Est, A.; Nikonov, G. I. Facile Catalytic Hydrosilylation of Pyridines. *Angew. Chem., Int. Ed.* **2011**, *50*, 1384−1387. (c) Petrushko, W. D.; Nikonov, G. I. Mono(hydrosilylation) of N-Heterocycles Catalyzed by $B(C_6F_5)_3$ and Silylium Ion. *Organometallics* **2020**, *39*, 4717−4722.

(13) Königs, C. D. F.; Klare, H. F. T.; Oestreich, M. Catalytic 1,4-Selective Hydrosilylation of Pyridines and Benzannulated Congeners. *Angew. Chem., Int. Ed.* **2013**, *52*, 10076−10079.

(14) Intemann, J.; Bauer, H.; Pahl, J.; Maron, L.; Harder, S. Calcium Hydride Catalyzed Highly 1,2-Selective Pyridine Hydrosilylation. *Chem.—Eur. J.* **2015**, *21*, 11452−11461.

(15) Jeong, J.; Park, S.; Chang, S. Iridium-Catalyzed Selective 1,2-Hydrosilylation of *N*-Heterocycles. *Chem. Sci.* **2016**, *7*, 5362−5370.

(16) Lortie, J. L.; Dudding, T.; Gabidullin, B. M.; Nikonov, G. I. Zinc-Catalyzed Hydrosilylation and Hydroboration of *N*-Heterocycles. *ACS Catal.* **2017**, *7*, 8454−8459.

(17) Pang, M.; Chen, J.-Y.; Zhang, S. J.; Liao, R. Z.; Tung, C. H.; Wang, W. G. Controlled Partial Transfer Hydrogenation of Quinolines by Cobalt-Amido Cooperative Catalysis. *Nat. Commun.* **2020**, *11*, 1249.

(18) Kaithal, A.; Chatterjee, B.; Gunanathan, C. Ruthenium Catalyzed Selective Hydroboration of Carbonyl Compounds. *Org. Lett.* **2015**, *17*, 4790−4793.

(19) Kisan, S.; Krishnakumar, V.; Gunanathan, C. Ruthenium-Catalyzed Anti-Markovnikov Selective Hydroboration of Olefins. *ACS Catal.* **2017**, *7*, 5950−5954.

(20) Kisan, S.; Krishnakumar, V.; Gunanathan, C. Ruthenium-Catalyzed Deoxygenative Hydroboration of Carboxylic Acids. *ACS Catal.* **2018**, *8*, 4772−4776.

(21) Kaithal, A.; Chatterjee, B.; Gunanathan, C. Ruthenium-Catalyzed Selective Hydroboration of Nitriles and Imines. *J. Org. Chem.* **2016**, *81*, 11153−11161.

(22) Chatterjee, B.; Gunanathan, C. Ruthenium Catalyzed Selective Hydrosilylation of Aldehydes. *Chem. Commun.* **2014**, *50*, 888−890.

(23) Chatterjee, B.; Gunanathan, C. Ruthenium-Catalysed Multicomponent Synthesis of Borasiloxanes. *Chem. Commun.* **2017**, *53*, 2515−2518.

(24) Kaithal, A.; Chatterjee, B.; Gunanathan, C. Ruthenium-Catalyzed Regioselective 1,4-Hydroboration of Pyridines. *Org. Lett.* **2016**, *18*, 3402−3405.

(25) Kaithal, A.; Kalsi, D.; Krishnakumar, V.; Pattanaik, S.; Bordet, A.; Leitner, W.; Gunanathan, C. Ruthenium-Catalyzed Selective Hydroboronolysis of Ethers. *ACS Catal.* **2020**, *10*, 14390−14397.

(26) Parr, R. G. Density Functional Theory of Atoms and Molecules. *Horizons of Quantum Chemistry*; Springer, 1980; pp 5−15.

(27) (a) Zhao, Y.; Truhlar, D. G. The M06 Suite of Density Functionals for Main Group Thermochemistry, Thermochemical Kinetics, Noncovalent Interactions, Excited States, and Transition Elements: Two New Functionals and Systematic Testing of Four M06-Class Functionals and 12 Other Functionals. *Theor. Chem. Acc.* **2008**, *120*, 215−241. (b) Zhao, Y.; Truhlar, D. G. Density Functionals With Broad Applicability in Chemistry. *Acc. Chem. Res.* **2008**, *41*, 157−167. (c) Cramer, C. J.; Truhlar, D. G. An SCF Solvation Model for the Hydrophobic Effect and Absolute Free Energies of Aqueous Solvation. *Science* **1992**, *256*, 213−217.

(28) (a) Remya, P. R.; Suresh, C. H. Hypercoordinate *β*-Carbon in Grubbs and Schrock Olefin Metathesis Metallacycles. *Dalton Trans.* **2015**, *44*, 17660−17672. (b) Remya, P. R.; Suresh, C. H. Mechanistic Studies on Acetylene Cyclotrimerization Catalyzed by Grubbs First and Second Generation Catalysts. *Mol. Catal.* **2017**, *441*, 63−71.

(29) Gordon, M. S.; Carroll, M. T.; Jensen, J. H.; Davis, L. P.; Burggraf, L. W.; Guidry, R. M. Nature of the Silicon-Nitrogen Bond in Silatranes. *Organometallics* **1991**, *10*, 2657−2660.

(30) (a) Bijina, P. V.; Suresh, C. H. Molecular Electrostatic Potential Reorganization Theory to Describe Positive Cooperativity in Noncovalent Trimer Complexes. *J. Phys. Chem. A* **2020**, *124*, 2231−2241. (b) Marín-Luna, M.; Alkorta, I.; Elguero, J. Cooperativity in Tetrel Bonds. *J. Phys. Chem. A* **2016**, *120*, 648−656. (c) Esrafili, M. D.; Mousavian, P. Strong Tetrel Bonds: Theoretical Aspects and Experimental Evidence. *Molecules* **2018**, *23*, 2642. (d) Cundari, T. R. Computational Studies of Transition Metal−Main Group Multiple Bonding. *Chem. Rev.* **2000**, *100*, 807−818.

(31) Mahmudov, K. T.; Gurbanov, A. V.; Guseinov, F. I.; Guedes da Silva, M. F. C. Noncovalent Interactions in Metal Complex Catalysis. *Coord. Chem. Rev.* **2019**, *387*, 32−46.

(32) Anglada, J. M.; Bo, C.; Bofill, J. M.; Crehuet, R.; Poblet, J. M. Inductive Effects in Neutral Pentacoordinated Silicon Compounds Containing a Si ← N Dative Bond. A Theoretical Study. *Organometallics* **1999**, *18*, 5584−5593.

(33) Bauzá, A.; Mooibroek, T. J.; Frontera, A. Tetrel-Bonding Interaction: Rediscovered Supramolecular Force? *Angew. Chem., Int. Ed.* **2013**, *52*, 12317−12321.

(34) Bauzá, A.; Seth, S. K.; Frontera, A. Tetrel Bonding Interactions at Work: Impact on Tin and Lead Coordination Compounds. *Coord. Chem. Rev.* **2019**, *384*, 107−125.

https://doi.org/10.1021/acscatal.1c01148
ACS Catal. 2021, 11, 5885−5893